

**Whole-body PET imaging in humans shows that  $^{11}\text{C}$ -PS13 is selective for  
cyclooxygenase-1 and can measure the in vivo potency of  
nonsteroidal anti-inflammatory drugs**

Min-Jeong Kim, Fernanda Juarez Anaya, Lester S. Manly, Jae-Hoon Lee, Jinsoo Hong,  
Stal Shrestha, Sanjay Telu, Katharine Henry, Jose A. Montero Santamaria, Jeih-San Liow,  
Paolo Zanotti-Fregonara, H. Umesha Shetty, Sami S. Zoghbi,  
Victor W. Pike, Robert B. Innis\*

Molecular Imaging Branch, National Institute of Mental Health, NIH, Bethesda, MD, USA

Submitted to *Journal of Nuclear Medicine* as an Original Research Article, February 2022.

Revised April 2022. Revised June 2022.

**Running title:** PET Imaging of COX-1

**Word Count:** 5158

**Correspondence**

Robert B. Innis, MD, PhD  
Molecular Imaging Branch,  
NIMH-NIH  
10 Center Drive, Rm.B1D43  
Bethesda, MD 20892  
Fax: +1-301-480-3610  
Tel: +1-301-594-1368  
Email: robert.innis@nih.gov

**First Author**

Min-Jeong Kim, MD, PhD  
Dept. Psychiatry and Behavioral Health,  
Stony Brook University School of Medicine  
101 Nicolls Road, HSC T10-041L  
Stony Brook, NY 11794  
Tel: +1-631-638-3154  
Fax: +1-631-444-1560  
Email: MinJeong.Kim@stonybrookmedicine.edu

## ABSTRACT

Both cyclooxygenase-1 (COX-1) and COX-2 convert arachidonic acid to prostaglandin H<sub>2</sub>, which has pro-inflammatory effects. The recently developed positron emission tomography (PET) radioligand <sup>11</sup>C-PS13 has excellent in vivo selectivity for COX-1 over COX-2 in non-human primates. This study sought to evaluate the selectivity of <sup>11</sup>C-PS13 binding to COX-1 in humans and assess the utility of <sup>11</sup>C-PS13 to measure the in vivo potency of nonsteroidal anti-inflammatory drugs (NSAIDs).

**Methods:** Baseline <sup>11</sup>C-PS13 whole-body PET scans were obtained in 26 healthy volunteers, followed by blocked scans with ketoprofen (n=8), celecoxib (n=8), or aspirin (n=8). Ketoprofen is a highly potent and selective COX-1 inhibitor, celecoxib is a preferential COX-2 inhibitor, and aspirin is a selective COX-1 inhibitor with a distinct mechanism that irreversibly inhibits substrate binding. Because blood cells, including platelets and white blood cells, also contain COX-1, <sup>11</sup>C-PS13 uptake inhibition from blood cells was measured in vitro and ex vivo (i.e., using blood obtained during PET scanning).

**Results:** High <sup>11</sup>C-PS13 uptake was observed in major organs with high COX-1 density, including the spleen, lungs, kidneys, and gastrointestinal tract. Ketoprofen (1-75mg p.o.) blocked uptake in these organs far more effectively than celecoxib (100-400mg p.o.). Based on the plasma concentration to inhibit 50% of the maximum radioligand binding in the spleen (in vivo *IC*<sub>50</sub>), ketoprofen (<0.24μM) was >10-fold more potent than celecoxib (>2.5μM) as a COX-1 inhibitor, consistent with the in vitro potencies of these drugs for inhibiting COX-1. Blockade of <sup>11</sup>C-PS13 uptake from blood cells acquired during the PET scans mirrored that in organs of the body. Aspirin (972-1,950mg p.o.) blocked such a small percentage of uptake that its in vivo *IC*<sub>50</sub> could not be determined.

**Conclusions:** <sup>11</sup>C-PS13 selectively binds to COX-1 in humans and can measure the in vivo potency of NSAIDs that competitively inhibit arachidonic acid binding to COX-1. These in vivo studies, which reflect the net effect of drug absorption and metabolism in all organs of the body, demonstrated that ketoprofen had unexpectedly high potency, that celecoxib substantially inhibited COX-1, and that aspirin acetylation of COX-1 did not block binding of the representative non-steroidal inhibitor <sup>11</sup>C-PS13.

**Keywords:** cyclooxygenase-1; positron emission tomography; inflammation; aspirin; celecoxib

**Registration:** NCT03324646 at <https://clinicaltrials.gov/>

## INTRODUCTION

The cyclooxygenase (COX) enzyme family is responsible for the biotransformation of arachidonic acid into various prostaglandins and thromboxanes that are major inflammatory mediators. The constitutively expressed COX-1 isoform has traditionally been thought to be responsible for maintaining the physiological integrity of major organs such as stomach and kidney as well as normal platelet function. In contrast, the inducible COX-2 isoform is thought to be associated with pathological responses to external injury or stimuli, including inflammation and pain (1). However, several studies suggest that COX-1 may play a previously underrecognized pro-inflammatory role in various pathologic conditions such as neurodegeneration (2,3), atherosclerosis (4), and carcinogenesis (5,6). In this respect, a selective positron emission tomography (PET) radioligand might serve to image COX as a surrogate marker for the development and progression of various diseases that have inflammation as one component of their pathogenesis. Any such radioligand would also be useful for measuring the target engagement of non-steroidal anti-inflammatory drugs (NSAIDs) tested in clinical trials for those diseases.

Previous studies from our laboratory reported initial PET results using the newly developed radioligand  $^{11}\text{C}$ -PS13 (Supplemental Fig.S1) in whole-body scans of nonhuman primates and human brain scans. PS13 is a highly potent COX-1 inhibitor ( $IC_{50}=1$  nM) and 1,000 times more selective for COX-1 than COX-2 (7). In non-human primates,  $^{11}\text{C}$ -PS13 showed selective binding to COX-1 over COX-2 in most major organs including the spleen, gastrointestinal tract, kidneys, and brain, as indicated by substantial blockade by COX-1 inhibitors and minimal blockade by COX-2 inhibitors (8). COX-1 is widely distributed in brain, with the highest concentrations found in the hippocampus, occipital cortex, and pericentral

cortex (9), and  $^{11}\text{C}$ -PS13 was found to be an excellent radioligand for measuring COX-1 in human brain. However, the pharmacologic selectivity of  $^{11}\text{C}$ -PS13 for COX-1 over COX-2 has not been confirmed in humans.

The present study used whole-body imaging in healthy human volunteers to investigate the selectivity of  $^{11}\text{C}$ -PS13 binding to COX-1 and to assess the ability of  $^{11}\text{C}$ -PS13 to measure the potency of COX-1 inhibitors. The COX-1 inhibitors ketoprofen (which is preferential for COX-1) and celecoxib (which is preferential for COX-2 but also inhibits COX-1 to a lower extent (10,11) were used. The effects of aspirin, which is 10- to 100-fold selective for COX-1 over COX-2 were also examined; notably, aspirin is the only clinically-used NSAID that irreversibly inhibits both COX-1 and COX-2 by acetylation of Ser-530, which is present adjacent to the binding site for the substrate, arachidonic acid (12). Although all other clinically used NSAIDs competitively inhibit arachidonic acid binding, it was unknown whether aspirin would block the binding of a small-molecule radioligand to this site.

## **Materials and Methods**

To determine the selectivity of binding to COX-1, the difference in  $^{11}\text{C}$ -PS13 uptake in major organs and blood cells was measured for baseline and/or blocked conditions using pharmacologic doses of ketoprofen, celecoxib, and aspirin in 26 healthy human volunteers. To explore the ability of  $^{11}\text{C}$ -PS13 to measure the potency of COX-1 inhibitors, the relationship between the blockade of  $^{11}\text{C}$ -PS13 binding and plasma concentrations of each blocker was examined after increasing oral doses. All participants gave informed consent in accordance with the National Institutes of Health Combined Neurosciences Institutional Review Board (Protocol

17-M-0179; NCT03324646). A detailed description of the methods and relevant citations (9,13-17) can be found in the Supplemental Materials.

## RESULTS

### Pharmacological effects, biodistribution, and dosimetry

<sup>11</sup>C-PS13 was intravenously injected once in 10 participants at baseline and twice in eight participants at baseline and after administration of ketoprofen (Supplemental Table S1). In another group of eight participants, <sup>11</sup>C-PS13 was injected three times: at baseline, after administration of celecoxib, and after administration of aspirin. The injected activity of 50 total scans was 693.1±51.9 MBq, corresponding to a molar dose of 0.14±0.07 nmol/kg. Neither the radioligand nor the blocking drugs caused any adverse effects, as assessed by participant self-report, blood pressure, pulse, temperature, respiratory rate, electrocardiogram, and basic laboratory tests.

The whole-body images were notable for early distribution in the blood pool (e.g., brain, thyroid gland, heart, and spleen), accumulation in target organs (e.g., spleen, brain, lung, and kidney), and apparent metabolism in the liver with visible excretion of activity in the gall bladder and small intestine (Supplemental Fig.S2). Radiation exposure was calculated from the organ distribution of radioactivity in the first 15 of 26 total participants (Supplemental Table S2). The mean effective dose of <sup>11</sup>C-PS13 derived from these 15 healthy volunteers was 4.6±0.6 μSv/MBq, resulting in radiation exposure of 3.4 mSv for an administered activity of 740 MBq (Supplemental Table S3). This dose is comparable to the mean dose of 21 other <sup>11</sup>C-labeled tracers used in human research (18), thus raising no unusual concerns about radiation safety. The

three organs receiving the highest radiation exposure ( $\mu\text{Sv}/\text{MBq}$ ) were the spleen ( $27.8\pm 1.1$ ), liver ( $9.8\pm 0.2$ ), and lungs ( $7.2\pm 0.1$ ).

### **Quantitation of organ uptake**

To determine whether the blocking drugs changed the concentration of radioligand in plasma, the average concentration of  $^{11}\text{C}$ -PS13 was compared at four timepoints (10, 30, 60, and 90 minutes) in the baseline and blocked scans. The plasma concentration of  $^{11}\text{C}$ -PS13 was slightly increased by ketoprofen ( $P=0.036$ ), but unchanged by celecoxib ( $P=0.484$ ) or aspirin ( $P=0.161$ ) (Supplemental Fig.S3). Because of the change induced by ketoprofen, organ uptake was normalized in each individual by their plasma concentration of radioligand between 10 and 90 minutes. Although this normalized value (i.e., the ratio of organ standardized uptake value (SUV) to plasma parent concentration ( $\text{SUV}/C_P$ )) was used, similar measurements of potency were found using only PET data (i.e., SUV) (data not shown). A detailed description of the method used to calculate and verify  $\text{SUV}/C_P$  can be found in the Supplemental Information (Supplemental Fig.S4). Data were not corrected for  $^{11}\text{C}$ -PS13 binding to plasma proteins for two reasons. First, the plasma free fraction was negligibly increased in blocked scans with ketoprofen ( $P=0.050$ ) and did not significantly increase in scans after blockade by celecoxib ( $P=0.208$ ) or aspirin ( $P=0.575$ ) (Supplemental Fig.S5). Second, our previous brain test-retest study suggested that the extremely low plasma free fraction value of  $^{11}\text{C}$ -PS13 with high variability could introduce unnecessary variance and perhaps even bias into subsequent analyses (9).

### **Selective binding to COX-1 in major organs**

As an overview of the blocking effects, the median and interquartile range (IQR) of the results were measured for each blocker, recognizing that varying doses were used for each drug. Ketoprofen, a COX-1 selective inhibitor, decreased  $^{11}\text{C}$ -PS13 organ uptake by the greatest amount (82% in the spleen (IQR 59-90%)) (Figs.1A, 2). Celecoxib, a COX-2 preferential inhibitor, blocked much less (25% in the spleen (IQR 2-35%)) (Figs.1B, 2), and aspirin had the weakest blocking effects (10% in the spleen (IQR 0-18%)) (Fig.2).

Blood cells, including platelets, monocytes, and erythrocytes, contain COX-1 and can be used as a measure of enzyme occupancy by NSAIDs (19-21). In the blood collected at four timepoints during the scans, cells were separated from the plasma, and the uptake of radioactivity in the cells was measured and normalized to the plasma concentration of  $^{11}\text{C}$ -PS13. Similar to uptake in organs of the body, uptake in the ex vivo cells showed selectivity for COX-1 over COX-2, and the order of percentage blockade was ketoprofen>celecoxib>aspirin (Fig.2). The percentage blockade measured in the ex vivo blood cells was highly consistent with the percentage blockade measured in the spleen with ketoprofen and celecoxib (Fig.3), a finding also observed in other organs ( $r$  range: 0.762-0.982).

### **In vivo potency of ketoprofen and celecoxib**

Both ketoprofen and celecoxib substantially blocked organ uptake and could be used to calculate their in vivo  $IC_{50}$  relative to their plasma concentrations. Because the spleen had the highest uptake at baseline and the greatest percentage blockade, it was used for these calculations, although similar results were found in other organs. The plasma concentration of ketoprofen was significantly and positively correlated with blocking of radioligand uptake in the

spleen ( $n=8$ ,  $r=0.976$ ,  $P<0.001$ ; Fig.4A) and all other organs ( $r\geq 0.762$ ). The plasma concentration of celecoxib was positively correlated with blocking in the spleen ( $n=8$ ,  $r=0.767$ ,  $P=0.037$ ; Fig.4B), but the correlation did not reach significance in other organs. From each correlation plot, the plasma concentration of drug that gives half-maximal spleen blockade (i.e., in vivo  $IC_{50}$ ) was estimated to be  $<0.24\mu\text{M}$  for ketoprofen and  $>2.5\mu\text{M}$  for celecoxib, which is a greater than 10-fold difference in potency. Greater precision could not be provided because ketoprofen rarely caused  $<50\%$  blockade, and celecoxib rarely caused  $>50\%$  blockade.

### **Brain Uptake**

Blockade by ketoprofen and celecoxib were examined using the subset of whole-body images that included the brain (Fig.5). The occupancy plot determines whether specific binding shown in all regions has the same occupancy, as would be expected for a single target (e.g., COX-1) with homogeneous affinity for the radioligand (22). Uptake in brain regions was quantified as  $\text{SUV}/C_P$ , like that for whole organs.

Three of the eight participants had minimal blockade of brain uptake by ketoprofen and thus could not be used for the occupancy plot analysis; specifically, the range of y-values in these three participants was too small to estimate an x-intercept. For the remaining five participants, the occupancy plot was reasonably linear— $r^2$  values ranged from 0.50 to 0.82—and the nondisplaceable uptake (x-intercept) was similar for four (1.06 to 1.96) but there was one outlier (0.14); values are expressed in units corresponding to  $\text{SUV}/C_P$ . Their occupancy showed a trend towards positive correlation with plasma ketoprofen concentration that did not reach statistical significance (Supplemental Fig. S6). Using these individually identified nondisplaceable uptake values, the average binding potential ( $BP_{\text{ND}}$ ) was  $1.25\pm 0.7$  for the first

four participants, with an outlying value of 48 in the last participant. The regions with the highest  $BP_{ND}$  values were the calcarine (1.88) and lingual gyrus (1.64) of the occipital region.

Interestingly, the two participants with the highest brain blockade by celecoxib (21% and 30%, respectively) also showed a reasonably linear occupancy plot, with  $BP_{ND}$  values estimated at 2.72 and 4.36.

### **Blockade by Aspirin**

Aspirin (972 to 1,950mg p.o.) blocked a small percentage of radioligand uptake in organs of the body. Even the highest doses of aspirin blocked only a modest percentage (<30%) of radioligand uptake in the spleen. The median blockade caused by aspirin in the spleen was only 10% (IQR 0-18%; Fig.2). Like the imaging results, ex vivo studies of blood cells harvested during the PET scans showed low blockade; the median blockade of blood cell uptake of  $^{11}C$ -PS13 was only 2% (IQR 0-50%). The median plasma aspirin concentration was 27 $\mu$ M (IQR 19-37 $\mu$ M), approximately 16-fold higher than the in vitro  $IC_{50}$  of aspirin.

To see whether aspirin was capable of blocking radioligand uptake if higher concentrations were achieved, whole blood cells collected from a healthy individual were incubated with aspirin (66 $\mu$ M) or ketoprofen (1.83 $\mu$ M), with each concentration being approximately 39-fold higher than the in vitro  $IC_{50}$  of the inhibitor. To assess the effect of the plasma itself, blood cells in plasma were compared, as were cells re-suspended in phosphate-buffered saline containing 0.4% dextrose. When incubated with plasma, aspirin blocked  $^{11}C$ -PS13 uptake by 23% and ketoprofen by 97% (Fig.6A). In contrast, when incubated in buffer, both aspirin and ketoprofen blocked a near-maximal amount: 90% and 93%, respectively (Fig.6B).

## DISCUSSION

Our results demonstrate that  $^{11}\text{C}$ -PS13 selectively binds to COX-1 in humans and that inhibition of its organ uptake provides a measure of the in vivo potency of NSAIDs for COX-1.  $^{11}\text{C}$ -PS13 uptake to COX-1 was high in major organs with abundant COX-1, such as the spleen, lungs, kidneys, gastrointestinal tract, and heart. Using percentage blockade of  $^{11}\text{C}$ -PS13 uptake in the spleen as the parameter of response, the in vivo potency of ketoprofen ( $IC_{50} < 0.24\mu\text{M}$ ) was more than 10-fold higher than that of celecoxib ( $IC_{50} > 2.5\mu\text{M}$ ). These in vivo potencies are consistent with the in vitro potencies of ketoprofen and celecoxib for COX-1 (10,23-25). In contrast, a single oral dose of aspirin (972-1,950mg) blocked little radioligand uptake in organs of the body or in ex vivo blood cells, consistent with its action at a site adjacent to but not directly in the binding site for small molecule inhibitors such as PS13 (Supplemental Fig.S1). Although the brain showed relatively smaller percentage blockade—probably due to the limited penetrance of blockers—the regional distribution of radioactivity was appropriate for that of COX-1 and was blocked by ketoprofen, such that the occupancy in all regions was, as expected, the same for high- and low-density regions. That is, the blockade was consistent with a single type of binding site (i.e., COX-1) and with all binding sites having the same affinity for the radioligand.

The  $^{11}\text{C}$ -PS13 PET images obtained under baseline and blocked conditions displayed the constitutive expression of COX-1 and were consistent with previous human postmortem studies (26) as well as with our in vivo studies in nonhuman primates (8). Although the major cell or tissue types with high binding of  $^{11}\text{C}$ -PS13 were not identified in this study, most of the organs that showed high specific binding were associated with the mononuclear phagocyte system, which includes blood monocytes and tissue macrophages in various organs such as the liver,

spleen, lungs, and brain (27). Similar to observations made in nonhuman primates (8), the spleen showed the highest specific binding to COX-1, which was likely due to stagnant blood cells encompassed within the spleen sinusoids. This is speculated from the remarkably similar values of percentage blockade between the spleen and ex vivo blood cells by ketoprofen and celecoxib (Fig.3); blood cells, particularly platelets, express abundant COX-1 (19-21).

The results of the present study are consistent with the high in vitro potency of ketoprofen to inhibit COX-1 and with the selectivity of ketoprofen and celecoxib for COX-1 versus COX-2. In this PET study, ketoprofen was found to have high in vivo potency, given that doses of only 5 mg po blocked more than 50% of organ uptake (Fig. 4A). By comparison, the typical therapeutic dose of ketoprofen is 75-300 mg (28). Regarding isozyme selectivity, the selectivity index (SI) of an NSAID for COX-1 equals the  $IC_{50}$  to inhibit COX-2 divided by that for COX-1, based on in vitro assay to inhibit prostaglandin production. Although the reported values of  $IC_{50}$  and SI are highly variable, the consensus is that ketoprofen is essentially selective for COX-1 (SI=8-61) (10,23), whereas celecoxib is only preferential for COX-2 (SI for COX-2=1.4-30) (23-25). Thus, high doses of celecoxib are expected to block a portion of radioligand binding to COX-1.

The very low blockade of radioligand uptake by aspirin is consistent with its two-step mechanism of action. Aspirin first weakly binds to the substrate (i.e., active) site of COX-1 and then acetylates the adjacent Ser-530, which irreversibly blocks access of bulky arachidonic acid to the substrate site (12). However, studies using COX-1 protein with amino acid substitutions suggest that this acetylation does not block access of inhibitors to the substrate binding site (12). The results of the present study directly confirm this speculation, given that the radioligand  $^{11}C$ -PS13, which itself is a small molecule inhibitor, was still able to bind even after exposure to

doses of aspirin that would be expected to fully acetylate COX-1 (Figs.2, 6A). The low affinity binding of aspirin to the substrate site was demonstrated in vitro with high concentrations of aspirin (66  $\mu$ M) in buffer rather than in plasma (Fig.6B). Plasma proteins decrease the effectiveness of aspirin by removing the drug from plasma water, thereby making it unavailable to diffuse to the target. Under these artificial conditions of no plasma proteins, aspirin was able to displace the radioligand. Thus, at pharmacological doses and concentrations, aspirin inhibited and irreversibly inactivated COX-1 without blocking access of inhibitors to the substrate binding site.

It should be noted that although celecoxib's inhibition of  $^{11}$ C-PS13 uptake may be caused by its cross-reactivity with COX-1, it may also be due to the cross-reactivity of PS13 with COX-2. The most direct way to address this possibility would have been to use another selective inhibitor, not just preferential, for COX-2; rofecoxib, which would have been ideal for this purpose, was withdrawn from clinical use because of its high incidence of adverse cardiovascular events (29). To our knowledge, celecoxib is the most COX-2-selective clinically available NSAID in the United States. However, to examine this issue, studies were performed in monkeys using MC1 as the COX-2-selective compound and PS13 as the COX-1-selective compound (8). The results indicated that  $^{11}$ C-PS13 was selective for COX-1 and had no measurable binding to COX-2.

The occupancy plot of brain uptake assumes that occupancy of specific binding is the same for all regions. Importantly, this analysis showed that ketoprofen enters the brain and displaces the radioligand from COX-1 (Fig.5). Both ketoprofen and our radioligand are highly selective for COX-1 over COX-2, and the fact that one blocked the other provides strong evidence that both selectively bind to COX-1. Interestingly, measurable occupancy was also

found in the two participants with the highest brain blockade by celecoxib. However, the occupancy plot also showed a limitation in our ability to measure brain uptake—i.e.,  $SUV/C_P$  data from 10 to 90 minutes—and  $C_P$  measured with venous samples. The noise and potential bias in these measurements presumably caused the poor identifiability of nondisplaceable uptake and  $BP_{ND}$ , which prevented us from obtaining consistent results in participants who received lower doses of the blockers. Future studies will explore whether full quantitation using continuous dynamic scans and arterial blood sampling might provide more accurate measurements.

The highly consistent blocking effect between ex vivo blood cells and the spleen suggests the potential utility of blood cells to evaluate COX-1 inhibitors in the future, even before PET images are obtained. As an example, the potency of a novel NSAID for COX-1 inhibition might be screened first with in vitro human blood cells using  $^{11}C$ -PS13 or a tritiated analog.

While the brain is protected from polar radiometabolites by the blood-brain barrier, most peripheral organs, including the spleen, have no such barrier. The percentage of contamination by radiometabolites in any organ will depend on the relative composition of three components: specific binding to the target receptor, nonspecific binding of the parent radioligand, and radiometabolites. We chose the spleen, which has a high percentage of specific binding (Fig. 2). However, most other organs (e.g., liver) will have a greater percentage of contamination by radiometabolites, which would underestimate the measured percentage blockade by blockers. To determine whether occupancy was stable in the spleen during the scan, we analyzed the time-stability of  $SUV/C_P$  with a method similar to the time-stability analysis in the brain (Supplemental Fig.S4F). No evidence of radiometabolite accumulation in the spleen over time was observed.

## **CONCLUSION**

<sup>11</sup>C-PS13 was selective for COX-1 in humans, as assessed via its distribution (which reflected that of COX-1 rather than COX-2) and by the much greater potency of ketoprofen compared to celecoxib to inhibit uptake in target organs. Using in vivo uptake in organs or ex vivo uptake in blood cells, <sup>11</sup>C-PS13 was able to measure the in vivo potencies for COX-1 of NSAIDs that act at the substrate binding site. Taken together, the results suggest that <sup>11</sup>C-PS13 can be used to determine whether any NSAID, except for aspirin, achieves adequate concentrations to inhibit COX-1 in the target organ, whether located centrally or in the periphery.

## **FINANCIAL DISCLOSURE**

This study was funded by the Intramural Research Program of the National Institute of Mental Health, National Institutes of Health (projects ZIAMH002795 and ZIAMH002793; NCT03324646).

## **DISCLAIMER**

The authors have no conflicts of interest, financial or otherwise.

## **ACKNOWLEDGEMENTS**

The authors thank the NIH PET Department (Chief, Peter Herscovitch) for performing the PET scanning and Ioline Henter (NIMH) for invaluable editorial assistance.

## **KEY POINTS**

**Question:** The recently developed positron emission tomography (PET) radioligand  $^{11}\text{C}$ -PS13 has excellent in vivo selectivity for cyclooxygenase-1 (COX-1) over COX-2 in non-human primates; this study sought to evaluate the selectivity of  $^{11}\text{C}$ -PS13 binding to COX-1 in humans and assess the utility of  $^{11}\text{C}$ -PS13 to measure the in vivo potency of nonsteroidal anti-inflammatory drugs (NSAIDs).

**Pertinent Findings:** High  $^{11}\text{C}$ -PS13 uptake was observed in major organs with high COX-1 density. Ketoprofen blocked uptake in these organs far more effectively than celecoxib, and aspirin only blocked a small percentage of uptake.

**Implications for Patient Care:** This study found that  $^{11}\text{C}$ -PS13 selectively binds to COX-1 in humans and can measure the in vivo potency of NSAIDs that competitively inhibit COX-1. Because COX-1 may play a pro-inflammatory role in the brain and periphery, a selective PET radioligand like  $^{11}\text{C}$ -PS13 could be used to image COX-1 as a surrogate marker for the development and progression of diseases marked by inflammation and measure the target engagement of NSAIDs as potential treatments.

## REFERENCES

1. Smith WL, Garavito RM, DeWitt DL. Prostaglandin endoperoxide H synthases (cyclooxygenases)-1 and -2. *J Biol Chem*. 1996;271:33157-33160.
2. O'Banion MK. Acute neuroinflammation and neurogenesis: a role for microglial COX-1. *Cell Cycle*. 2011;10:3819-3820.
3. Calvello R, Panaro MA, Carbone ML, et al. Novel selective COX-1 inhibitors suppress neuroinflammatory mediators in LPS-stimulated N13 microglial cells. *Pharmacol Res*. 2012;65:137-148.
4. Praticò D, Tillmann C, Zhang Z-B, Li H, FitzGerald GA. Acceleration of atherogenesis by COX-1-dependent prostanoid formation in low density lipoprotein receptor knockout mice. *Proc Natl Acad Sci USA*. 2001;98:3358-3363.
5. Ranger GS. Current concepts in colorectal cancer prevention with cyclooxygenase inhibitors. *Anticancer Res*. 2014;34:6277-6282.
6. Yu Z-H, Zhang Q, Wang Y-D, et al. Overexpression of cyclooxygenase-1 correlates with poor prognosis in renal cell carcinoma. *Asian Pac J Cancer Prev*. 2013;14:3729-3734.
7. Shrestha S, Singh P, Cortes-Salva MY, et al. 3-Substituted 1,5-diaryl-1 H-1,2,4-triazoles as prospective PET radioligands for imaging brain COX-1 in monkey. Part 2: Selection and evaluation of [(11)C]PS13 for quantitative imaging. *ACS Chem Neurosci*. 2018;9:2620-2627.
8. Kim MJ, Shrestha SS, Cortes M, et al. Evaluation of two potent and selective PET radioligands to image COX-1 and COX-2 in rhesus monkeys. *J Nucl Med*. 2018;59:1907-1912.
9. Kim MJ, Lee JH, Juarez Anaya F, et al. First-in-human evaluation of [(11)C]PS13, a novel PET radioligand, to quantify cyclooxygenase-1 in the brain. *Eur J Nucl Med Mol Imaging*. 2020;47:3143-3151.
10. Cryer B, Feldman M. Cyclooxygenase-1 and cyclooxygenase-2 selectivity of widely used nonsteroidal anti-inflammatory drugs. *Am J Med*. 1998;104:413-421.
11. Rimon G, Sidhu RS, Lauver DA, et al. Coxibs interfere with the action of aspirin by binding tightly to one monomer of cyclooxygenase-1. *Proc Natl Acad Sci USA*. 2010;107:28-33.

12. Blobaum AL, Marnett LJ. Structural and functional basis of cyclooxygenase inhibition. *J Med Chem.* 2007;50:1425-1441.
13. Gandelman MS, Baldwin RM, Zoghbi SS, Zea-Ponce Y, Innis RB. Evaluation of ultrafiltration for the free-fraction determination of single photon emission computed tomography (SPECT) radiotracers: beta-CIT, IBF, and iomazenil. *J Pharm Sci.* 1994;83:1014-1019.
14. Hines CS, Liow JS, Zanotti-Fregonara P, et al. Human biodistribution and dosimetry of <sup>11</sup>C-CUMI-101, an agonist radioligand for serotonin-1a receptors in brain. *PLoS One.* 2011;6:e25309.
15. Kanegawa N, Collste K, Forsberg A, et al. In vivo evidence of a functional association between immune cells in blood and brain in healthy human subjects. *Brain Behav Immun.* 2016;54:149-157.
16. Singh P, Shrestha S, Cortes-Salva MY, et al. 3-Substituted 1,5-diaryl-1 H-1,2,4-triazoles as prospective PET radioligands for imaging brain COX-1 in monkey. Part 1: Synthesis and pharmacology. *ACS Chem Neurosci.* 2018;9:2610-2619.
17. Zoghbi SS, Shetty HU, Ichise M, et al. PET imaging of the dopamine transporter with 18F-FECNT: a polar radiometabolite confounds brain radioligand measurements. *J Nucl Med.* 2006;47:520-527.
18. Zanotti-Fregonara P, Innis RB. Suggested pathway to assess radiation safety of <sup>11</sup>C-labeled PET tracers for first-in-human studies. *Eur J Nucl Med Mol Imaging.* 2012;39:544-547.
19. Belton O, Byrne D, Kearney D, Leahy A, Fitzgerald DJ. Cyclooxygenase-1 and -2-dependent prostacyclin formation in patients with atherosclerosis. *Circulation.* 2000;102:840-845.
20. Rocca B, Secchiero P, Celeghini C, et al. Modulation of the expression and activity of cyclooxygenases in normal and accelerated erythropoiesis. *Exp Hematol.* 2004;32:925-934.
21. Brideau C, Kargman S, Liu S, et al. A human whole blood assay for clinical evaluation of biochemical efficacy of cyclooxygenase inhibitors. *Inflamm Res.* 1996;45:68-74.

- 22.** Cunningham VJ, Rabiner EA, Slifstein M, Laruelle M, Gunn RN. Measuring drug occupancy in the absence of a reference region: the Lassen plot re-visited. *J Cereb Blood Flow Metab.* 2010;30:46-50.
- 23.** Warner TD, Giuliano F, Vojnovic I, Bukasa A, Mitchell JA, Vane JR. Nonsteroid drug selectivities for cyclo-oxygenase-1 rather than cyclo-oxygenase-2 are associated with human gastrointestinal toxicity: a full in vitro analysis. *Proc Natl Acad Sci USA.* 1999;96:7563-7568.
- 24.** Chan CC, Boyce S, Brideau C, et al. Rofecoxib [Vioxx, MK-0966; 4-(4'-methylsulfonylphenyl)-3-phenyl-2-(5H)-furanone]: a potent and orally active cyclooxygenase-2 inhibitor. Pharmacological and biochemical profiles. *J Pharmacol Exp Ther.* 1999;290:551-560.
- 25.** Tacconelli S, Capone ML, Sciulli MG, Ricciotti E, Patrignani P. The biochemical selectivity of novel COX-2 inhibitors in whole blood assays of COX-isozyme activity. *Curr Med Res Opin.* 2002;18:503-511.
- 26.** Zidar N, Odar K, Glavac D, Jerse M, Zupanc T, Stajer D. Cyclooxygenase in normal human tissues--is COX-1 really a constitutive isoform, and COX-2 an inducible isoform? *J Cell Mol Med.* 2009;13:3753-3763.
- 27.** van Furth R, Cohn ZA, Hirsch JG, Humphrey JH, Spector WG, Langevoort HL. The mononuclear phagocyte system: a new classification of macrophages, monocytes, and their precursor cells. *Bull World Health Organ.* 1972;46:845-852.
- 28.** FDA. [https://www.accessdata.fda.gov/drugsatfda\\_docs/label/2007/019816s011lbl.pdf](https://www.accessdata.fda.gov/drugsatfda_docs/label/2007/019816s011lbl.pdf). Accessed December 13, 2021.
- 29.** Sibbald B. Rofecoxib (Vioxx) voluntarily withdrawn from market. *CMAJ.* 2004;171:1027-1028.

## **Figure Legends**

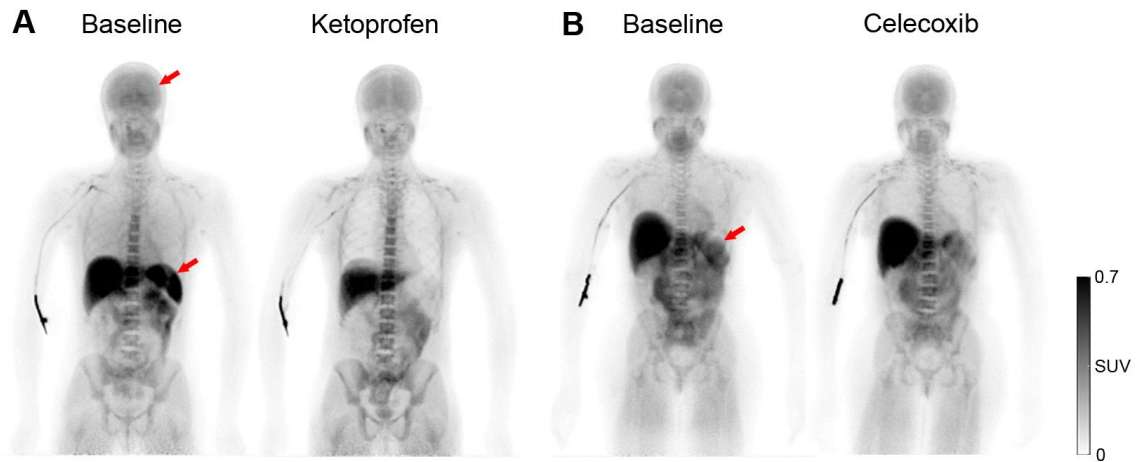


**Figure 1.** Planar images of healthy volunteers after injection of  $^{11}\text{C}$ -PS13 under baseline conditions and after administration of blockers. (A) Under baseline conditions and after oral administration of ketoprofen (0.35mg/kg). Upper arrow=brain; lower arrow=spleen. (B) Under baseline conditions and after oral administration of celecoxib (6.55mg/kg). Arrow=spleen. The images were averaged from 10 to 90 minutes and compressed from anterior to posterior.

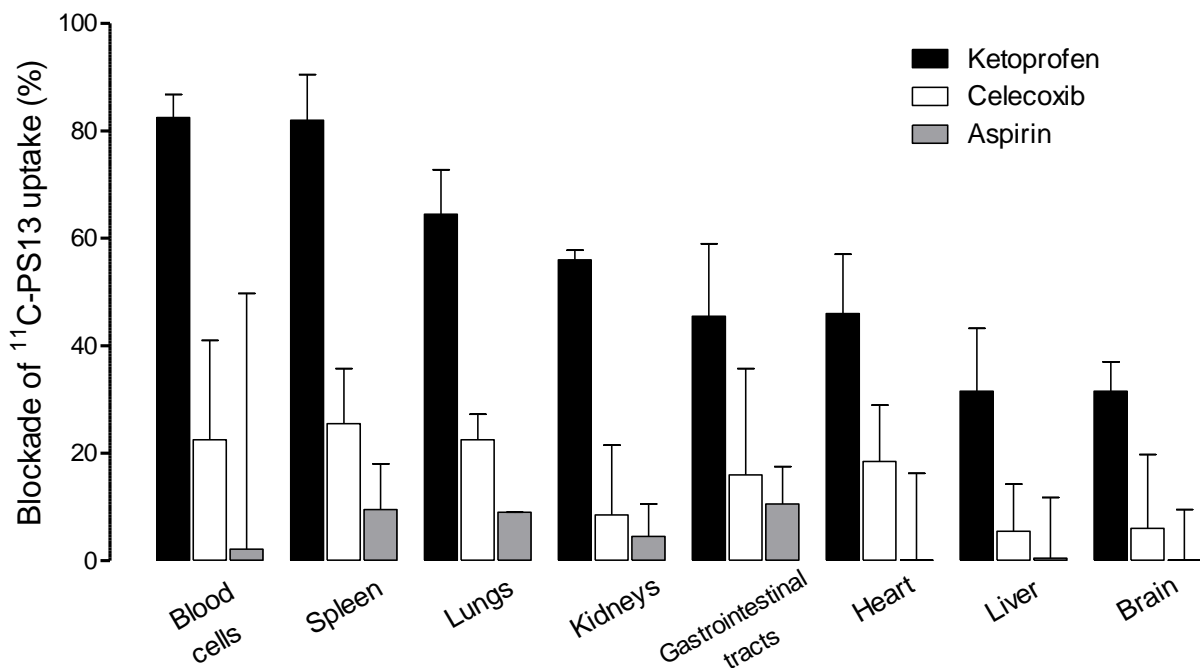


**Figure 2.** The percentage blockade of  $^{11}\text{C}$ -PS13 binding in major organs and ex vivo blood cells after pharmacological doses of ketoprofen, celecoxib, and aspirin ( $n=8$  in each condition). The administered dose ranged from 1-75mg for ketoprofen, 100-400mg for celecoxib, and 972-1,950mg for aspirin. Data are presented by median and interquartile range. Binding in the organs from the PET images was measured as a tissue to plasma ratio from 10 to 90 minutes—i.e., concentration of radioactivity in the organ divided by the concentration of parent radioligand in plasma ( $\text{SUV}/C_P$ ). For the ex vivo studies, blood was withdrawn at 10, 30, 60, and 90 minutes. Binding of  $^{11}\text{C}$ -PS13 was then measured as a ratio of the concentration of radioligand within the cells to that in the plasma. We refer to this binding as the distribution volume of the blood cells ( $V_{BC}$ ).

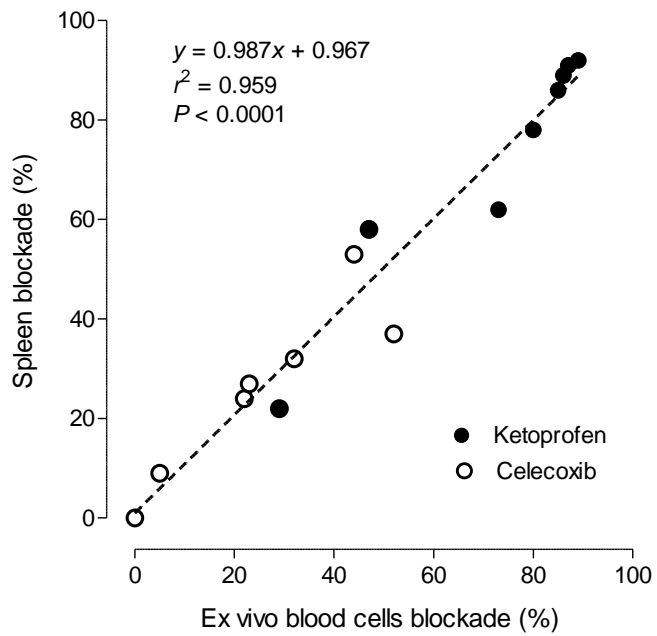


**Figure 3.** Consistency between the percentage blockade of ex vivo blood cells and the spleen by ketoprofen and celecoxib, calculated using SUV/C<sub>P</sub>.

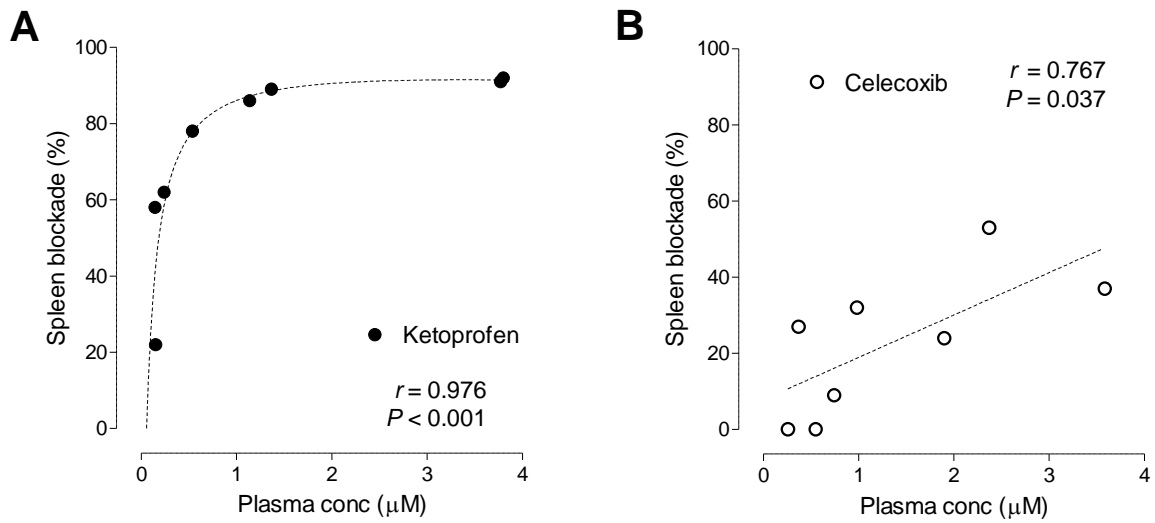


**Figure 4.** Dose-response plots of the percentage blockade in the spleen after oral administration of ketoprofen (A) or celecoxib (B). For ketoprofen, the single oral doses ranged from 1 to 75 mg. The three left-most points (i.e., those with the lowest plasma concentrations of ketoprofen) were from participants who received either 1 or 5 mg po. For celecoxib, the single oral doses ranged from 100 to 400 mg, and one participant received the maximal dose.  $r$ =Spearman’s correlation coefficient.

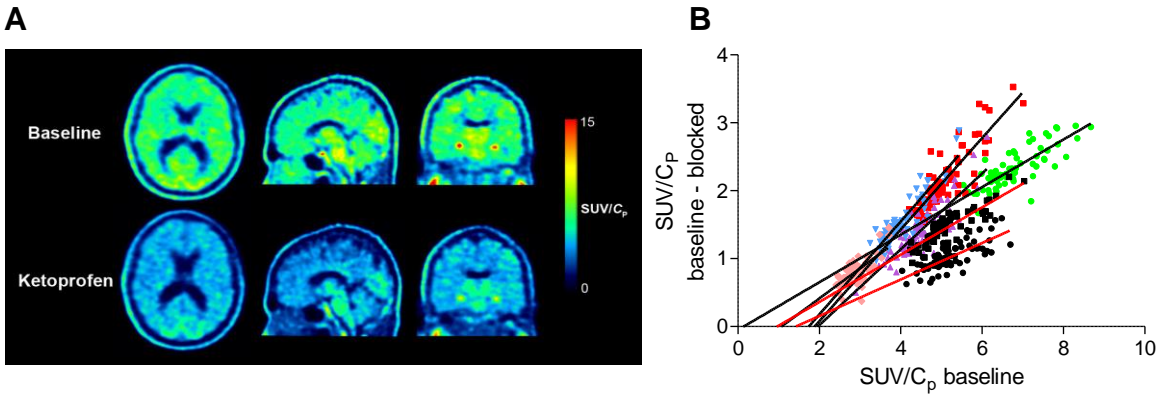


**Figure 5.** Blockade by ketoprofen in the brain of a representative participant (A), and occupancy plots of participants after blockade by ketoprofen (colored points in five participants) or celecoxib (black points in two participants) (B). (B) These plotted seven participants had the greatest blockade among all participants. Each point represents a brain region, and each color represents an individual participant. The occupancy (i.e., slope) of cyclooxygenase-1 (COX-1) was about 54% for ketoprofen and 31% for celecoxib. Binding was measured as SUV/C<sub>p</sub>.

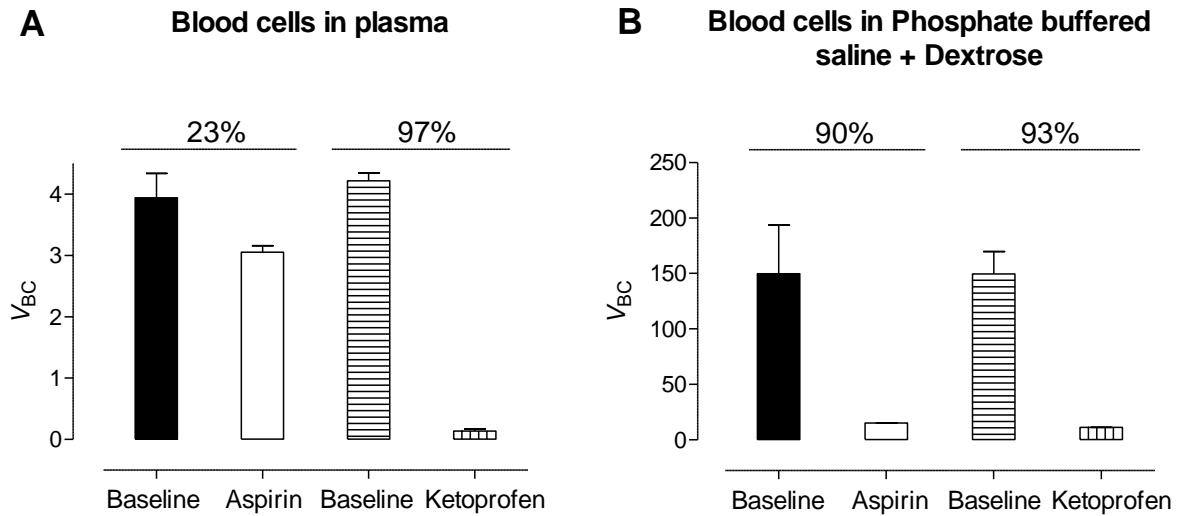
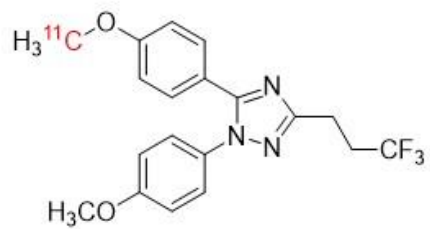


**Figure 6.** In vitro experiment with incubated whole blood cells collected from a healthy participant. High doses of aspirin and ketoprofen were used; each concentration was approximately 39-fold higher than the in vitro  $IC_{50}$ . The bar graph presents the mean and standard error of the mean from six divided samples with separate centrifuge and gamma-counting. Percentage blockade is presented by mean percentage blockade from six samples of each condition. Binding of  $^{11}C$ -PS13 was measured as the concentration of radioligand within the cells to that in the plasma. We refer to this binding as the distribution volume of the blood cells ( $V_{BC}$ ).

## Graphical Abstract



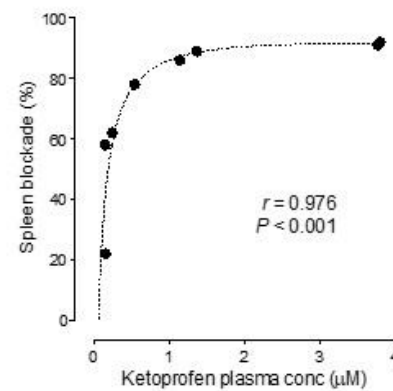
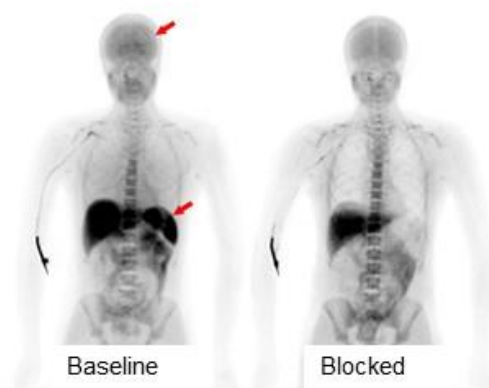
**$^{11}\text{C}$ -PS13**

In vitro  $IC_{50}$  for COX-1 = 1 nM

In vitro  $IC_{50}$  for COX-2 > 1,000 nM



## Ketoprofen



In vivo  $IC_{50}$  for COX-1 < 0.24  $\mu\text{M}$

## **SUPPLEMENTAL INFORMATION**

### **Radiopharmaceutical Preparation**

<sup>11</sup>C-PS13 was prepared as previously described (1), with a molar activity of 91±45 GBq/μmol at the time of injection under our Investigational New Drug Application 136,241. The radiochemical purity was 99.3±0.8%, with these and subsequent data expressed as mean±SD.

### **Participants**

Demographic characteristics for the 26 healthy volunteers who participated in this study can be found in Supplemental Table S1. A baseline whole-body biodistribution study was conducted in all participants, and the baseline whole-body imaging data for 15 of the 26 participants were then used for dosimetry analyses. Whole-body scans blocked with ketoprofen were obtained from eight participants, and whole-body scans blocked with celecoxib and aspirin were obtained from another eight participants. All participants were medically healthy based on their history, physical examination, blood and urine laboratory testing, and electrocardiogram. None of the participants had taken any kind of NSAIDs for two weeks or aspirin for four weeks prior to the PET scans. All participants gave informed consent in accordance with the National Institutes of Health Combined Neurosciences Institutional Review Board (Protocol 17-M-0179; NCT03324646).

### **Blocking studies using ketoprofen and celecoxib**

For blocking studies, baseline and blocked whole-body PET scans were obtained either on different days or on the same day with the radioligand injections separated by four hours; the

first scan served as the baseline scan, and the second scan served as the blocked scan. Before each blocking scan, a single oral dose of either ketoprofen, celecoxib, or aspirin was administered. The administered dose ranged over 1-75 mg for ketoprofen, 100-400 mg for celecoxib, and 972-1,950 mg for aspirin. The time intervals between administration of the blocking drugs and the radioligand injection, as well as between administration of the blocking drugs and blood sampling are shown in Supplemental Table S1. The time intervals were determined based on the time to peak drug concentration of each blocker. Venous blood was collected before and after each PET scan to measure the mean plasma levels of the blocking drugs. The time intervals for aspirin were shorter than those for ketoprofen or celecoxib because of the significantly faster absorption rate after p.o. administration of aspirin.

### **PET data acquisition and blood analyses**

Whole-body PET scans were obtained on a Biograph mCT scanner (Siemens Healthineers; Erlangen, Germany) in three dimensions; CT scans for attenuation correction were acquired in two dimensions before radioligand injection. Following a one-minute intravenous bolus injection of  $^{11}\text{C}$ -PS13, whole-body dynamic emission scans in 7-8 different bed positions were obtained from head to upper thigh for 90 minutes in 11-12 frames (e.g.,  $4 \times 0.25$  min,  $3 \times 0.5$  min,  $3 \times 1$  min,  $1 \times 2$  min, and  $1 \times 4$  min for seven bed positions). PET images were reconstructed with ordered subset expectation maximization (OSEM) with time of flight (TOF) and resolution recovery using the following parameters: three iterations, 21 subsets, 400 matrix size, 1.0 zoom, and no post-filter. Each scan image was visually inspected for any significant motion that could have affected the quality of data.

To determine the plasma radioligand concentrations, venous blood samples were drawn from the antecubital vein concurrently with PET scans at about 10, 30, 60, and 90 minutes after radioligand injection. In each sample, the concentration of parent radioligand was measured after separating plasma from whole blood as previously described (2). The plasma free fraction ( $f_p$ ) of  $^{11}\text{C}$ -PS13 was also measured in triplicate for each scan and with pooled human arterial plasma that had previously been collected for purposes of standardization and stored at  $-80\text{ }^\circ\text{C}$ . The latter served as the standard for normalization across scans. Measurements were performed by ultrafiltration through membrane filters, as previously described (3).

To investigate the binding of  $^{11}\text{C}$ -PS13 in blood cells, the percentage blockade in ex vivo blood cells was also calculated in the scans. Blood cell radioactivity concentrations were calculated as follows (4):

$$C_{\text{BC}} = C_{\text{P}} + (C_{\text{WB}} - C_{\text{P}})/H$$

$C_{\text{BC}}$ ,  $C_{\text{WB}}$ , and  $C_{\text{P}}$  are the concentrations of radioactivity (cpm/mL) in blood cells, whole blood, and plasma, respectively, and  $H$  is hematocrit.

Similar to the brain uptake measurements, distribution volume of the blood cells ( $V_{\text{BC}}$ ) was defined as:

$$V_{\text{BC}} = C_{\text{BC}}/C_{\text{P}}$$

The within-subject difference in the plasma levels of  $^{11}\text{C}$ -PS13 between different study conditions was compared using the Wilcoxon signed-rank test with significance level set at  $P < 0.05$  (IBM SPSS Version 28; Chicago, IL, USA).

### **Baseline biodistribution and dosimetry analyses**

Whole-body PET images were calibrated to Bq/mL and analyzed using PMOD 3.9 (PMOD Technologies Ltd., Zurich, Switzerland). Based on anatomical information from the corresponding CT scan, 12 source organs (brain, heart, liver, gall bladder, stomach, spleen, lungs, kidneys, small intestine, large intestine, lumbar spine, and urinary bladder) were identified on whole-body images, and the time-activity curves were obtained. Subsequent dosimetry analyses were performed as previously published (5). The software program OLINDA/EXM 1.1 was used to calculate radiation equivalent doses according to the Medical Internal Radiation Dose using the 70-kg adult male model.

### **Image analyses of baseline and blocked scans**

Based on anatomical information from the corresponding CT scan, seven organs of interest (brain, lungs, heart, liver, spleen, kidneys, and gastrointestinal tract) were identified on whole-body baseline and blocked scans, and time-activity curves were obtained. The activity of each organ was expressed as standardized uptake value (SUV), calculated by dividing the measured radioactivity concentration by the injected radioactivity and body weight. To quantify uptake, the mean concentration of radioactivity in each organ was calculated from 10 to 90 minutes. The first 10 minutes were avoided because they are highly influenced by drug delivery and blood volume.

To correct for the potential influence of the blocking drugs on metabolism and clearance of the radioligand, additional analyses were conducted using a simplified ratio method, with venous blood samples drawn at four timepoints during the baseline and blocked scans. The ratio of organ SUV to plasma parent concentration ( $SUV/C_p$ ) was calculated from 10-90 minutes

using venous blood data from four timepoints (10, 30, 60, and 90 minutes). The percentage blockade in each organ was calculated as follows:

$$\text{Percentage blockade (\%)} = \frac{\text{Baseline SUV}/C_P - \text{Blocked SUV}/C_P}{\text{Baseline SUV}/C_P} \times 100(\%)$$

Where SUV/ $C_P$  represents tissue to plasma ratio of mean SUV between 10 and 90 minutes.

### **Verification of the simplified ratio method with venous blood**

In order to determine whether the SUV/ $C_P$  calculated from limited venous blood sampling could be used for quantitation of  $^{11}\text{C}$ -PS13 binding, additional analyses were conducted in  $^{11}\text{C}$ -PS13 brain scan data obtained for a previously published study (6). Eleven blood data sets from six participants were available to compare the arterial and venous plasma concentrations of parent radioligand. Twenty full data sets of brain and arterial blood from 10 participants were available to compare the simplified ratio method and the full quantitative method, both using arterial blood. Seven full data sets of brain and both venous and arterial blood from four participants were available to compare the simplified ratio method using venous blood and the full quantitative method using arterial blood. Correlations between two different methods were analyzed using Spearman's rank-order correlation method. Bland-Altman plot was used to show mean versus percent difference of the results from the two different methods and to provide a comprehensive visual assessment of the data by Prism 5.02 (GraphPad Software, Inc., La Jolla, CA, USA). The time-stability of the SUV/ $C_P$  calculated from limited venous blood sampling was evaluated from 30 to 90 minutes. The ratio of the spleen SUV/ $C_P$  values from the truncated scan to that from the 90-minute measurement was computed for baseline and blocked condition by ketoprofen in eight participants. The results are presented in Supplemental Figure S4.

## **Brain occupancy plot analysis**

To assess whether ketoprofen blocks the uptake of  $^{11}\text{C}$ -PS13 in the brain, an occupancy plot was used to analyze differences in brain uptake at baseline and after blockade by ketoprofen in the eight participants who were scanned with whole-body acquisitions. The brain images were extracted from the whole-body scans, normalized on the Montreal Neurological Institute (MNI) template, and segmented into 71 regions using the automated anatomical labelling (AAL) atlas implemented in PMOD 4.2.

Although the occupancy plot was not based on absolute quantitation of total distribution volume ( $V_T$ ),  $\text{SUV}/C_P$  was used as a surrogate  $V_T$  and nondisplaceable uptake (x-intercept; surrogate  $V_{ND}$ ) was obtained that was consistent in four out of five participants. Binding potential ( $BP_{ND}$ ) was calculated from the ratio of specific uptake  $V_S (=V_T - V_{ND})$  and nondisplaceable uptake ( $V_{ND}$ ) in each brain region.

## **Analysis of dose-response relationship**

The plasma concentration of each blocker was measured using the LC-MS/MS method. Because the spleen showed the highest baseline  $^{11}\text{C}$ -PS13 binding and the highest percentage blockade with all three blockers, percentage blockade of  $^{11}\text{C}$ -PS13 in the spleen was used as the major parameter representing the blocking effects of COX-1 binding in major target organs. The correlation between plasma ketoprofen or celecoxib concentrations and percentage blockade of  $^{11}\text{C}$ -PS13 in the spleen was analyzed using Spearman's rank-order correlation in Prism 5.02.

### **In vitro blood cell experiments**

To observe the effects of different in vitro conditions on the ability of aspirin and ketoprofen to block  $^{11}\text{C}$ -PS13 binding in blood cells, an additional in vitro experiment was conducted using whole blood collected from a separate healthy volunteer. After anticoagulation and determination of the hematocrit by microhematocrit centrifugation, half of the whole blood was centrifuged, and the plasma was replaced by phosphate buffered saline (PBS) containing 0.4% dextrose. Each whole blood sample and the sample replaced by PBS and dextrose was divided into four aliquots. Either aspirin (66  $\mu\text{M}$ ), ketoprofen (1.83  $\mu\text{M}$ ), or sham solvent for each blocker (DMSO $\pm$ saline) was added to each sample and incubated at 37 °C for 20 minutes.  $^{11}\text{C}$ -PS13 (10  $\mu\text{Ci}/5.0\text{ mL}$ ) was then added, followed by additional incubation at 37 °C for 20 minutes. All samples were then assayed in an automatic gamma-counter.

## REFERENCES

1. Singh P, Shrestha S, Cortes-Salva MY, et al. 3-Substituted 1,5-diaryl-1 H-1,2,4-triazoles as prospective PET radioligands for imaging brain COX-1 in monkey. Part 1: Synthesis and pharmacology. *ACS Chem Neurosci*. 2018;9:2610-2619.
2. Zoghbi SS, Shetty HU, Ichise M, et al. PET imaging of the dopamine transporter with <sup>18</sup>F-FECNT: a polar radiometabolite confounds brain radioligand measurements. *J Nucl Med*. 2006;47:520-527.
3. Gandelman MS, Baldwin RM, Zoghbi SS, Zea-Ponce Y, Innis RB. Evaluation of ultrafiltration for the free-fraction determination of single photon emission computed tomography (SPECT) radiotracers: beta-CIT, IBF, and iomazenil. *J Pharm Sci*. 1994;83:1014-1019.
4. Kanegawa N, Collste K, Forsberg A, et al. In vivo evidence of a functional association between immune cells in blood and brain in healthy human subjects. *Brain Behav Immun*. 2016;54:149-157.
5. Hines CS, Liow JS, Zanotti-Fregonara P, et al. Human biodistribution and dosimetry of <sup>11</sup>C-CUMI-101, an agonist radioligand for serotonin-1a receptors in brain. *PLoS One*. 2011;6:e25309.
6. Kim MJ, Lee JH, Juarez Anaya F, et al. First-in-human evaluation of [<sup>11</sup>C]PS13, a novel PET radioligand, to quantify cyclooxygenase-1 in the brain. *Eur J Nucl Med Mol Imaging*. 2020;47:3143-3151.

**Supplemental Table S1.** Participant information for each study component

	Baseline biodistribution (n=26)	Dosimetry (n=15)	Blocking with ketoprofen (n=8)	Blocking with celecoxib* (n=8)	Blocking with aspirin* (n=8)
Age (years)	34.9±13.5	30.7±8.8	39.8±15.6	35.4±13.7	35.4±13.7
Sex (F:M)	13:13	10:5	1:7	5:3	5:3
Body weight (kg)	71.2±14.0	72.0±14.5	75.2±10.9	69.5±13.8	69.7±14.0
Time interval between blocker administration and radioligand injection (hours)	-	-	2.2±0.2	2.2±0.3	1.2±0.3
Time interval between blocker administration and blood sampling (hours)	-	-	2.0±0.2 and 3.8±0.2	2.0±0.4 and 3.8±0.3	1.1±0.3 and 3.0±0.5

\*The same individuals participated in both studies.

**Supplemental Table S2.** Residence times of source organs and remainder of body in 15 healthy volunteers

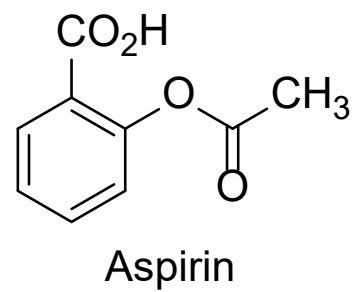
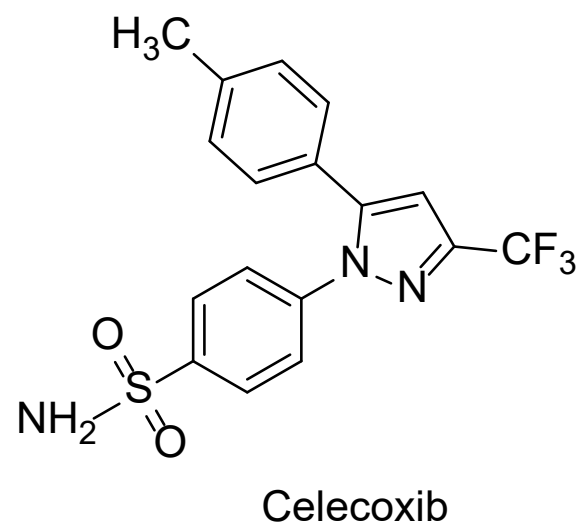
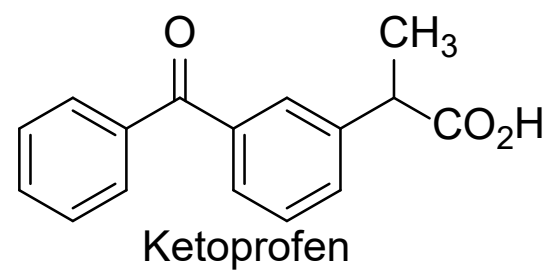
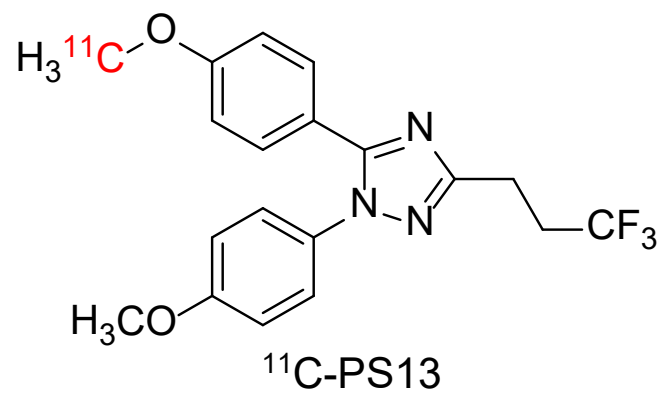
Organ	Residence time (hour)	COV (%)
Brain	0.0182	17.5
Heart	0.0084	14.0
Liver	0.0529	17.0
Kidneys	0.0041	26.4
Lungs	0.0234	17.3
Stomach	0.0031	32.8
Spleen	0.0180	43.4
Red marrow	0.0355	44.2
Gall bladder	0.0007	80.5
Small intestine	0.0244	25.2
ULI wall	0.0038	86.0
Urinary bladder	0.0013	55.6
Remainder of body	0.2964	8.1
Total	0.4902	

Abbreviations: ULI: upper large intestine

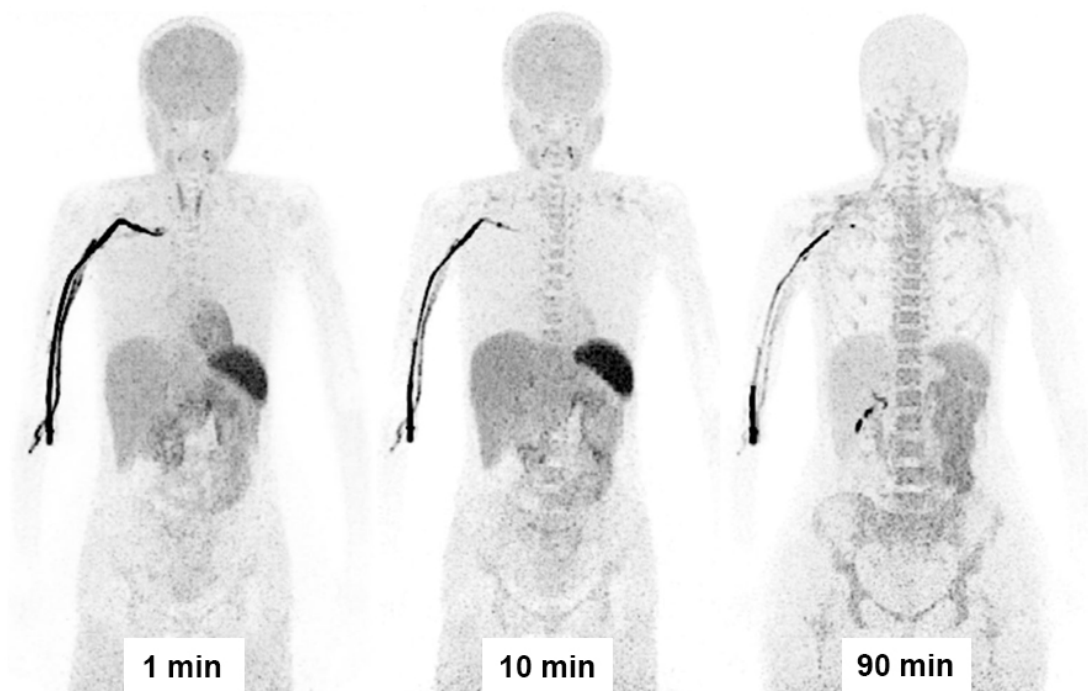
**Supplemental Table S3.** Radiation dose estimates for <sup>11</sup>C-PS13 in 15 healthy volunteers

Organ	Dose (μSv/MBq)	COV (%)
Spleen	27.84	41.0
Liver	9.80	15.3
Lungs	7.22	14.3
Small intestine	5.67	61.1
Red marrow	5.66	27.2
Kidneys	5.43	21.0
Heart wall	5.25	7.0
Gallbladder wall	5.07	27.2
Osteogenic cells	4.99	18.8
Brain	4.59	15.5
ULI wall	4.43	54.1
Pancreas	3.54	7.9
Stomach wall	3.45	26.0
Adrenals	3.23	3.1
Urinary bladder wall	2.95	16.7
Ovaries	2.84	21.7
Total body	2.77	3.4
Uterus	2.62	9.1
LLI wall	2.52	7.3
Testes	2.41	56.6
Thymus	2.36	3.3
Muscle	2.16	4.5
Thyroid	2.09	5.3
Breasts	1.94	3.6
Skin	1.69	5.2
Effective Dose	4.60	2.5

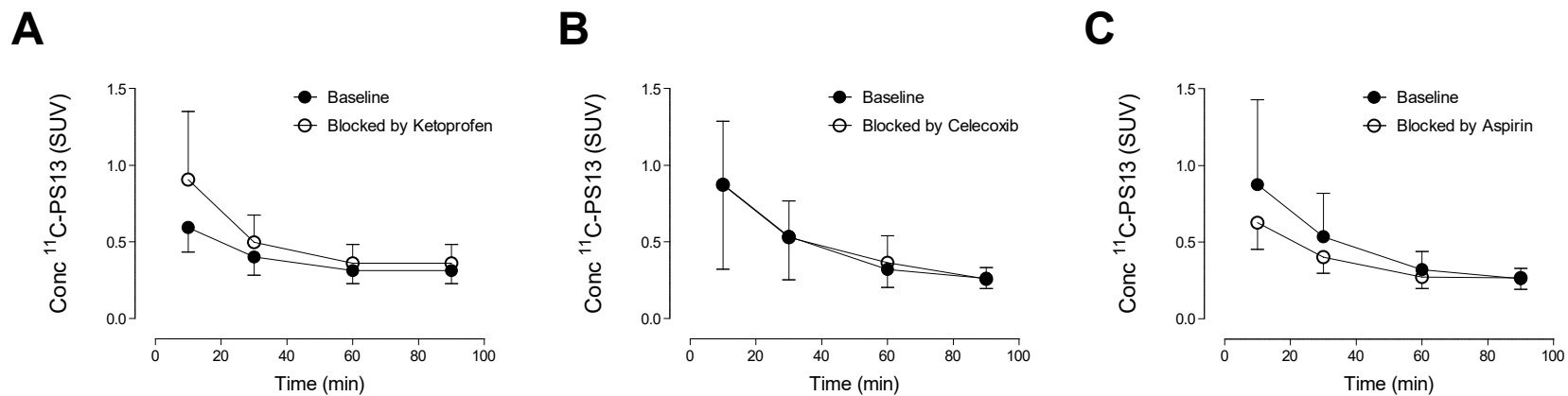
Abbreviations: LLI: lower large intestine; ULI: upper large intestine



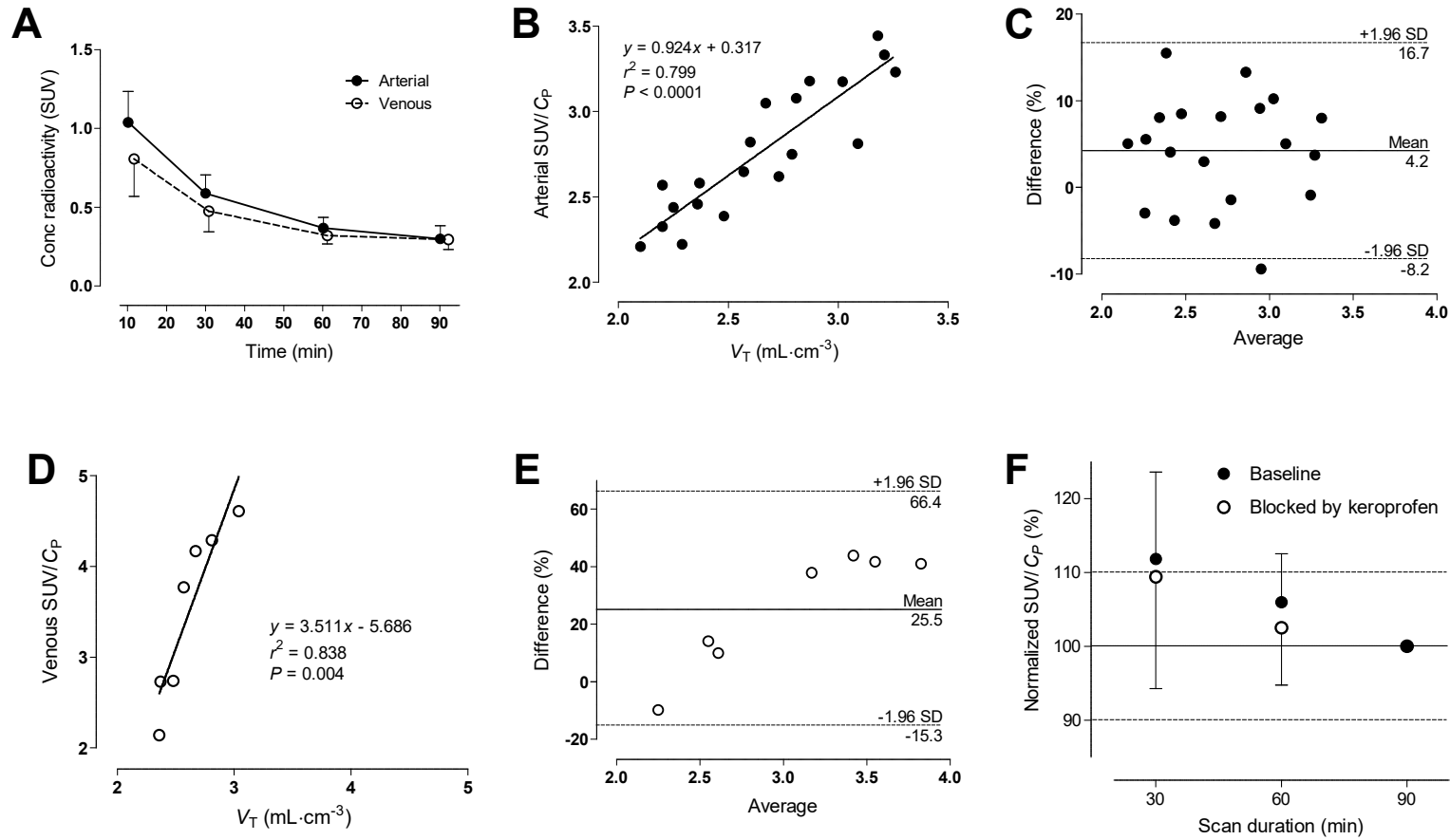
**Supplemental Figure S1.** Chemical structures of  $^{11}\text{C}$ -PS13 and blockers.



**Supplemental Figure S2.** Biodistribution of radioactivity in a healthy female participant after injecting 623 MBq of  $^{11}\text{C}$ -PS13. The three images are on the same display scale.

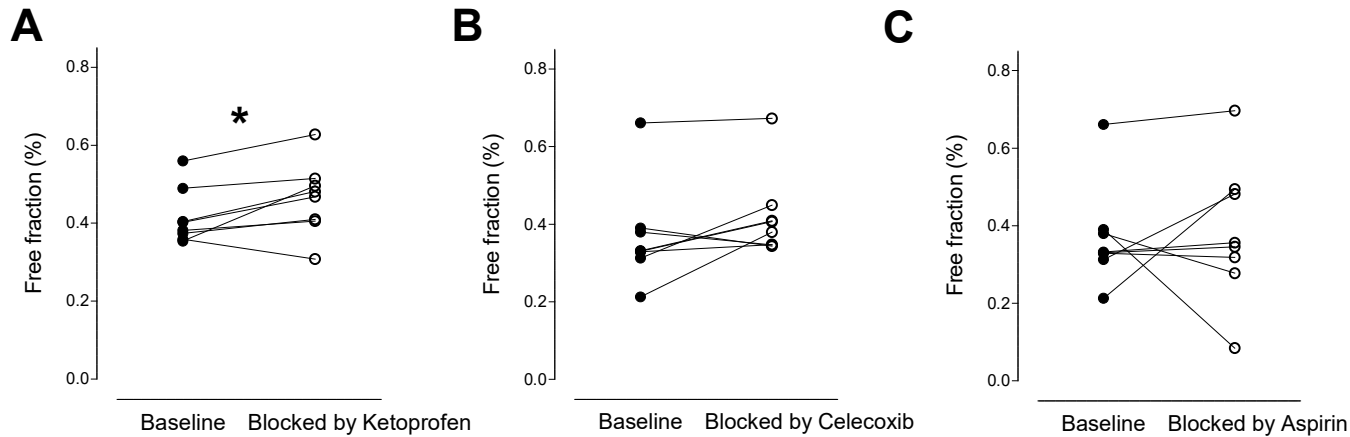


**Supplemental Figure S3.** Comparison of plasma  $^{11}\text{C}$ -PS13 concentrations between baseline and blocked conditions with ketoprofen (A), celecoxib (B), and aspirin (C) ( $n=8$  in each group). Blocking with ketoprofen significantly increased mean plasma  $^{11}\text{C}$ -PS13 concentration ( $P=0.036$ ), while blocking with celecoxib or aspirin did not.

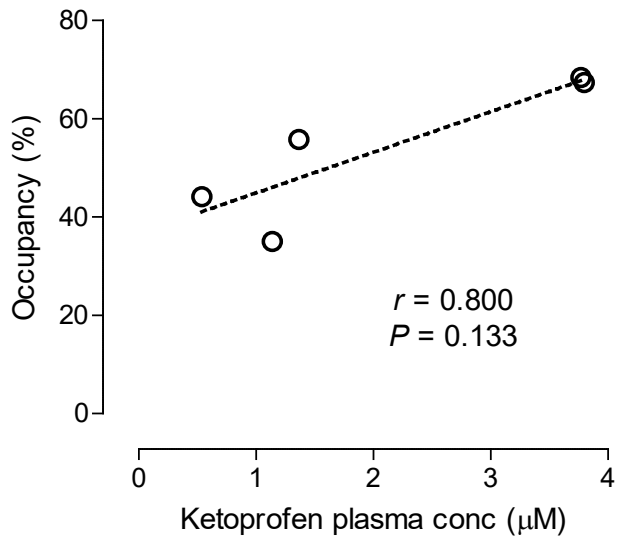


**Supplemental Figure S4.** Verification of a simplified ratio method using limited venous blood samples in the brain and spleen. (A) Comparison of plasma parent concentration between arterial and venous blood at four timepoints (n=11). Data are mean ± SD. Venous plasma tended to show lower levels than arterial plasma, although the difference was smaller at later timepoints. (B) The standardized

uptake value (SUV) ratio calculated using four timepoints of arterial plasma concentration (arterial SUV/ $C_P$ ) showed excellent correlation with total distribution volume ( $V_T$ ) calculated using the two-tissue compartment model and full arterial data in the whole brain (n=20;  $r=0.912$ ,  $P<0.001$ ). (C) Bland-Altman plot comparing arterial SUV/ $C_P$  and  $V_T$  in the whole brain. Although arterial SUV/ $C_P$  showed higher values than  $V_T$  by 4.2% on average, the percent difference was fairly distributed within the  $\pm 1.96$  SD range. (D) The SUV ratio calculated using four timepoints of venous plasma concentration (venous SUV/ $C_P$ ) showed excellent correlation with  $V_T$  calculated by the two-tissue compartment model using full arterial data in the whole brain (n=7;  $r=1.000$ ,  $P<0.001$ ). (E) Bland-Altman plot for comparison between venous SUV/ $C_P$  and  $V_T$  in the whole brain. The percent difference was fairly distributed within the  $\pm 1.96$  SD range with a mean difference of 25.5%. (F) Time-stability analysis of venous SUV/ $C_P$  of the spleen under baseline and blocked conditions by ketoprofen (n=8). Each venous SUV/ $C_P$  calculated at 30 and 60 minutes was normalized to the value measured at 90 minutes. Data are mean  $\pm$  SD. The plot shows no evidence of radiometabolite accumulation in the spleen.



**Supplemental Figure S5.** The within-subject comparison of  $^{11}\text{C}$ -PS13 plasma free fraction between baseline and blocked conditions with ketoprofen (A), celecoxib (B), and aspirin (C) ( $n=8$  in each). Blocking with ketoprofen slightly increased free fraction with borderline significance ( $0.42\pm 0.07\%$  at baseline and  $0.46\pm 0.09\%$  at blocked;  $*P=0.050$ ), while blocking with celecoxib or aspirin showed no significant difference from baseline ( $0.37\pm 0.12\%$  at baseline and  $0.42\pm 0.10\%$  at blocked with celecoxib;  $0.37\pm 0.12\%$  at baseline and  $0.38\pm 0.17\%$  at blocked with aspirin).



**Supplemental Figure S6.** The correlation plot between plasma concentration of ketoprofen and brain occupancy (%) in five participants. The occupancy—the slope in each occupancy plot—could only be estimated from those five of the eight total participants who received higher doses of ketoprofen. A trend towards positive correlation was observed that did not reach statistical significance.  $r$ =Spearman's correlation coefficient.